

Fig. 1 Development of CRISPR-GEMs. (A) Schematic of CRISPR-GEMs lentiviral constructs comprising of a dCas9 moiety fused to one of multiple epigenetic-modifying domains: KRAB, HDAC8, SIRT6 or SETDB2 (core) or their catalytically impaired counterparts (denoted by “mutant”). CRISPR-GEM: CRISPR-guided epigenome modifier; gRNA: guide RNA. (B) Expression of target genes DKK1, IGFBPL1 and MLNR 3 days post-transfection in HDAC8-KO HEK293T upon co-transfection of 2 gRNAs and CRISPR-GEMs. mRNA expression relative to cells transfected by gRNA-only (No effector) is represented by mean±SEM (n=3 for DKK1 and IGFBPL1 n=2 for MLNR). The differences between no effector and CRISPR-GEMs were analyzed by two-way Welch’s test. *P<0.05, **P<0.01, ***P<0.001.

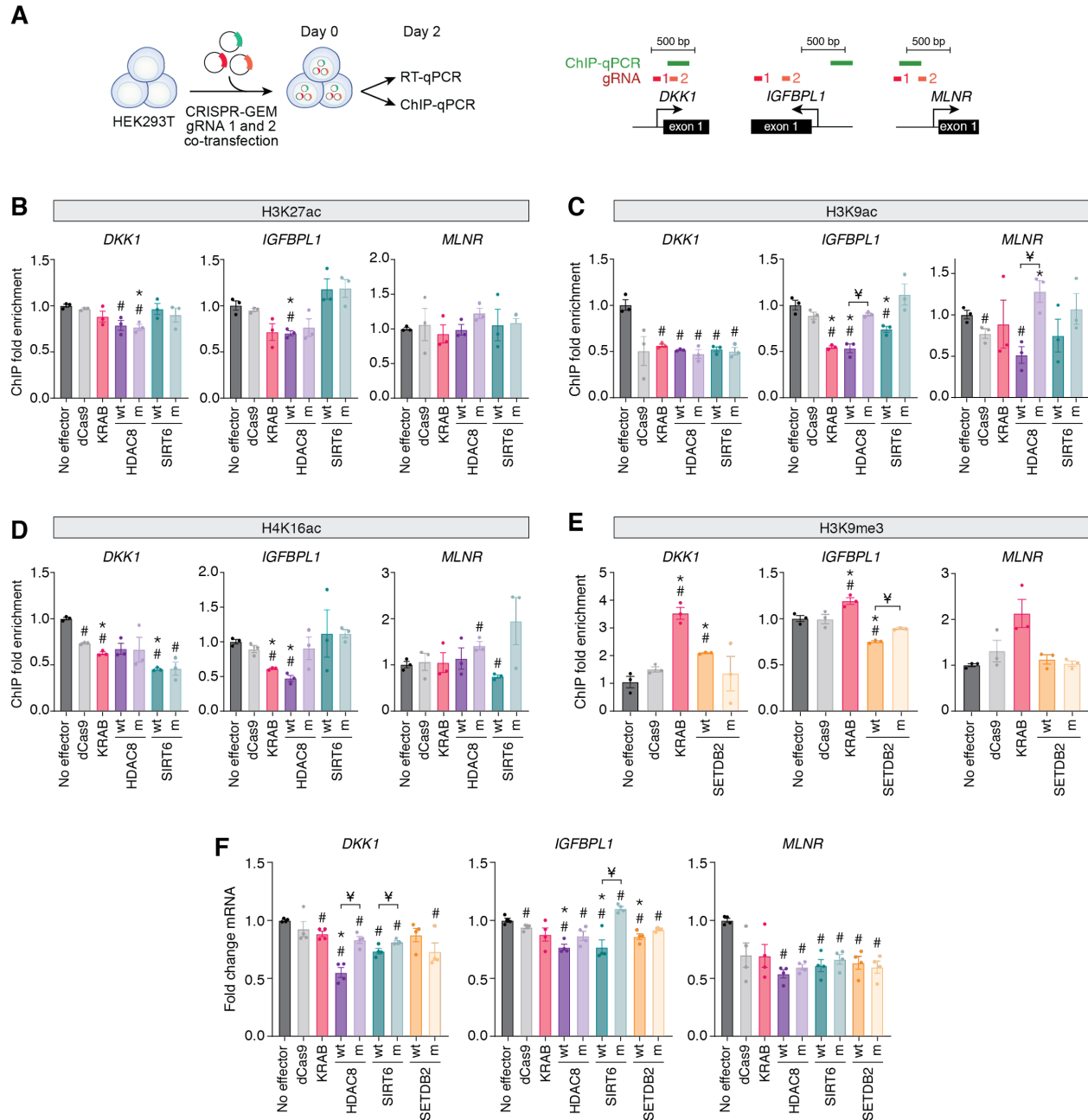


Fig. 2 Characterizing the effects of CRISPR-GEMs on gene expression and histone marks on Day 2. (A) Left, a diagram of the experimental setup. Right, a schematic of the three targeted loci, depicting the locations of the gRNAs and regions that were used for ChIP-qPCR relative to the target gene. (B-E) ChIP-qPCR fold enrichment of assayed marks (H3K27ac, H3K9ac, H4K16ac and H3K9me3, respectively) in tested loci DKK1, IGFBPL1 and MLNR 2 days

post-transfection in wildtype HEK293T upon co-transfection of 2 gRNAs and CRISPR-GEMs.

(F) Relative DKK1, IGFBPL1 and MLNR mRNA levels resulting from dCas9-GEMs compared to no effector control or dCas9 with no GEM was determined by RT-qPCR in wildtype HEK293T cells 2 days post-co-transfection with plasmids expressing the indicated dCas9 fusions and the two gRNAs targeting the indicated gene promoter. No effector: cells transfected by gRNA-only. wt: wildtype; m: mutant. n=3-4 biologically independent samples (cell cultures) for all conditions. Data are presented as mean \pm s.e.m relative to cells transfected by gRNA-only (no effector). Two-way Welch's t-test was applied for all statistical comparisons. [#]*P* < 0.05 versus no effector control; ^{*}*P* < 0.05 versus dCas9; [‡]*P* < 0.05 between CRISPR-GEMs and their respective mutant counterparts; ns: not significant.

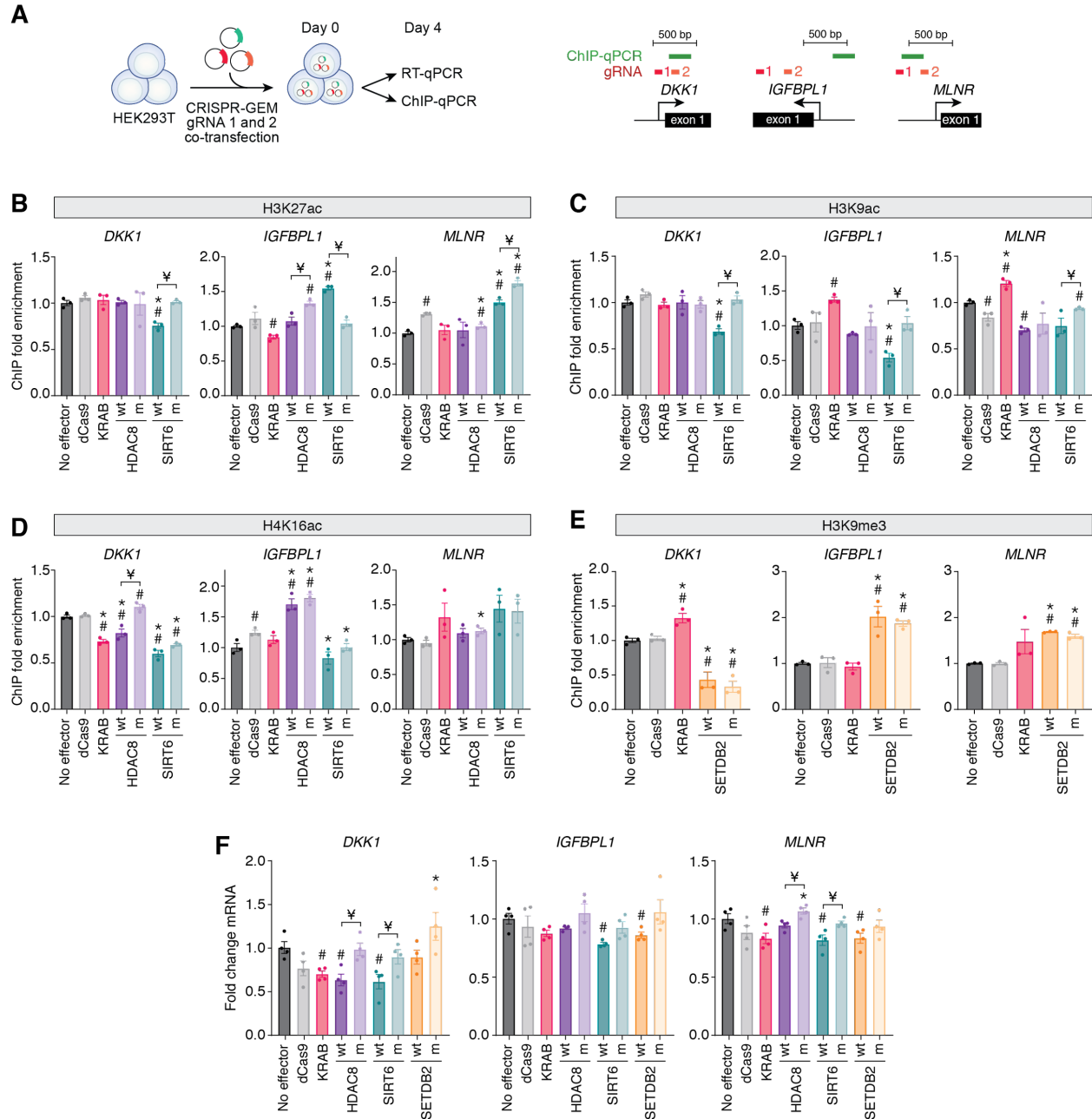


Fig. 3 Characterizing the effects of CRISPR-GEMs on gene expression and histone marks on Day 4. (A) Left, a diagram of the experimental setup. Right, a schematic of the three targeted loci, depicting the locations of the gRNAs and regions that were used for ChIP-qPCR relative to the target gene. (B-E) ChIP-qPCR fold enrichment of assayed marks (H3K27ac, H3K9ac, H4K16ac and H3K9me3, respectively) in tested loci DKK1, IGFBPL1 and MLNR 4 days

post-transfection in wildtype HEK293T upon co-transfection of 2 gRNAs and CRISPR-GEMs.

(F) Relative DKK1, IGFBPL1 and MLNR mRNA levels resulting from dCas9-GEMs compared to no effector control or dCas9 with no GEM was determined by RT-qPCR in wildtype HEK293T cells 4 days post-co-transfection with plasmids expressing the indicated dCas9 fusions and the two gRNAs targeting the indicated gene promoter. No effector: cells transfected by gRNA-only. wt: wildtype; m: mutant. n=3-4 biologically independent samples (cell cultures) for all conditions. Data are presented as mean \pm s.e.m relative to cells transfected by gRNA-only (no effector). Two-way Welch's t-test was applied for all statistical comparisons. [#]*P* < 0.05 versus no effector control; ^{*}*P* < 0.05 versus dCas9; [‡]*P* < 0.05 between CRISPR-GEMs and their respective mutant counterparts; ns: not significant.

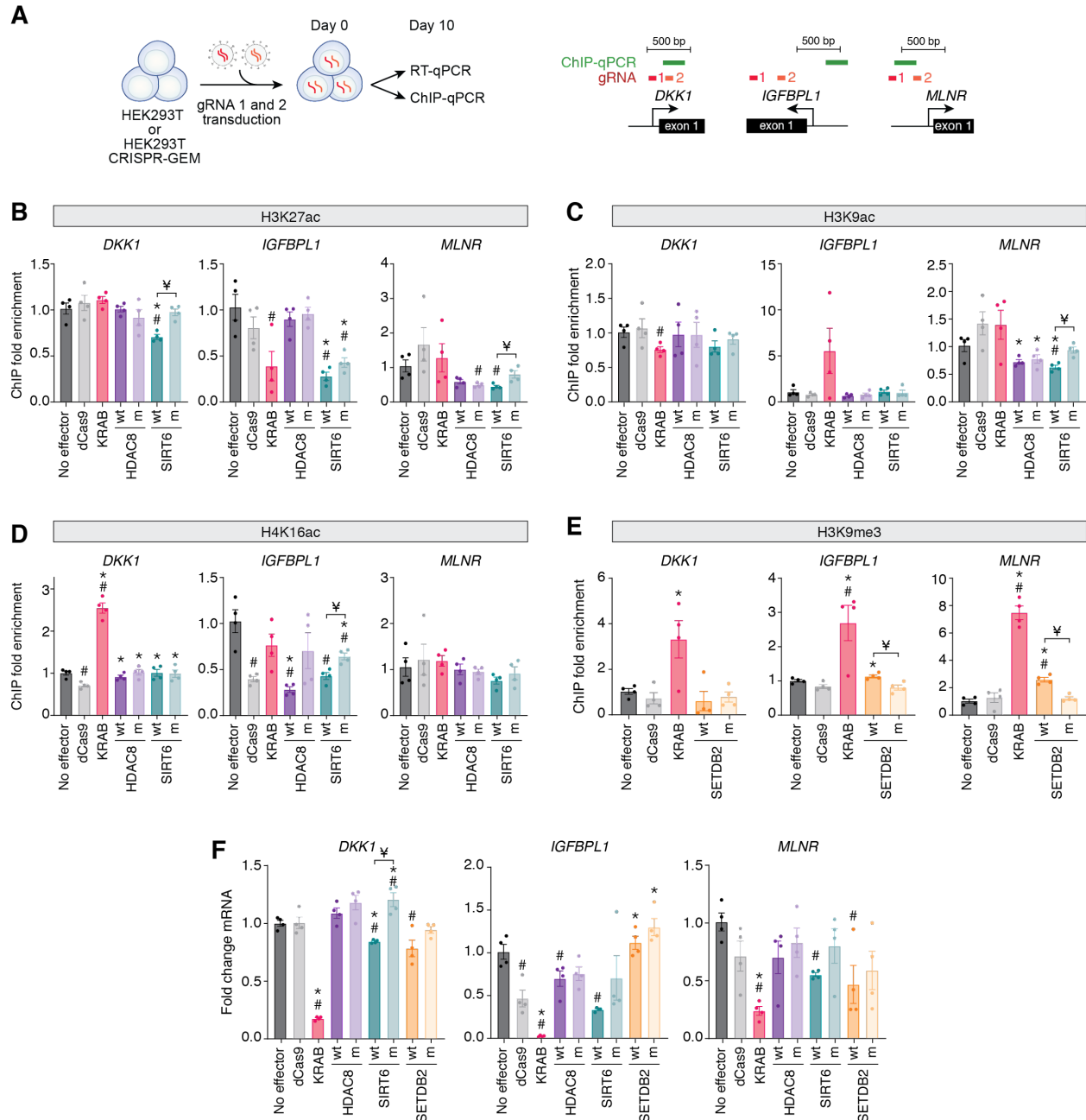


Fig. 4 Characterizing the effects of CRISPR-GEMs on gene expression and histone marks under long-term lentiviral expression (10 days). (A) Left, a diagram of the experimental setup. Right, a schematic of the three targeted loci, depicting the locations of the gRNAs and regions that were used for ChIP-qPCR relative to the target gene. (B-E) ChIP-qPCR fold enrichment of assayed marks (H3K27ac, H3K9ac, H4K16ac and H3K9me3, respectively) in tested loci DKK1,

IGFBPL1 and MLNR 10 days post-transduction of HEK293T polyclonal CRISPR-GEM expressing cells with viruses expressing two gRNAs targeting the indicated gene promoter. (F) Relative DKK1, IGFBPL1 and MLNR mRNA levels resulting from dCas9-GEMs compared to no effector control or dCas9 with no GEM was determined by RT-qPCR in HEK293T polyclonal CRISPR-GEM expressing cells 10 days post-transduction with viruses expressing two gRNAs targeting the indicated gene promoter. No effector: cells transfected by gRNA-only. wt: wildtype; m: mutant. n=4-5 biologically independent samples (cell cultures) for all conditions. Data are presented as mean \pm s.e.m relative to cells transfected by gRNA-only (no effector). Two-way Welch's t-test was applied for all statistical comparisons. [#]*P* < 0.05 versus no effector control; ^{*}*P* < 0.05 versus dCas9; [‡]*P* < 0.05 between CRISPR-GEMs and their respective mutant counterparts; ns: not significant.

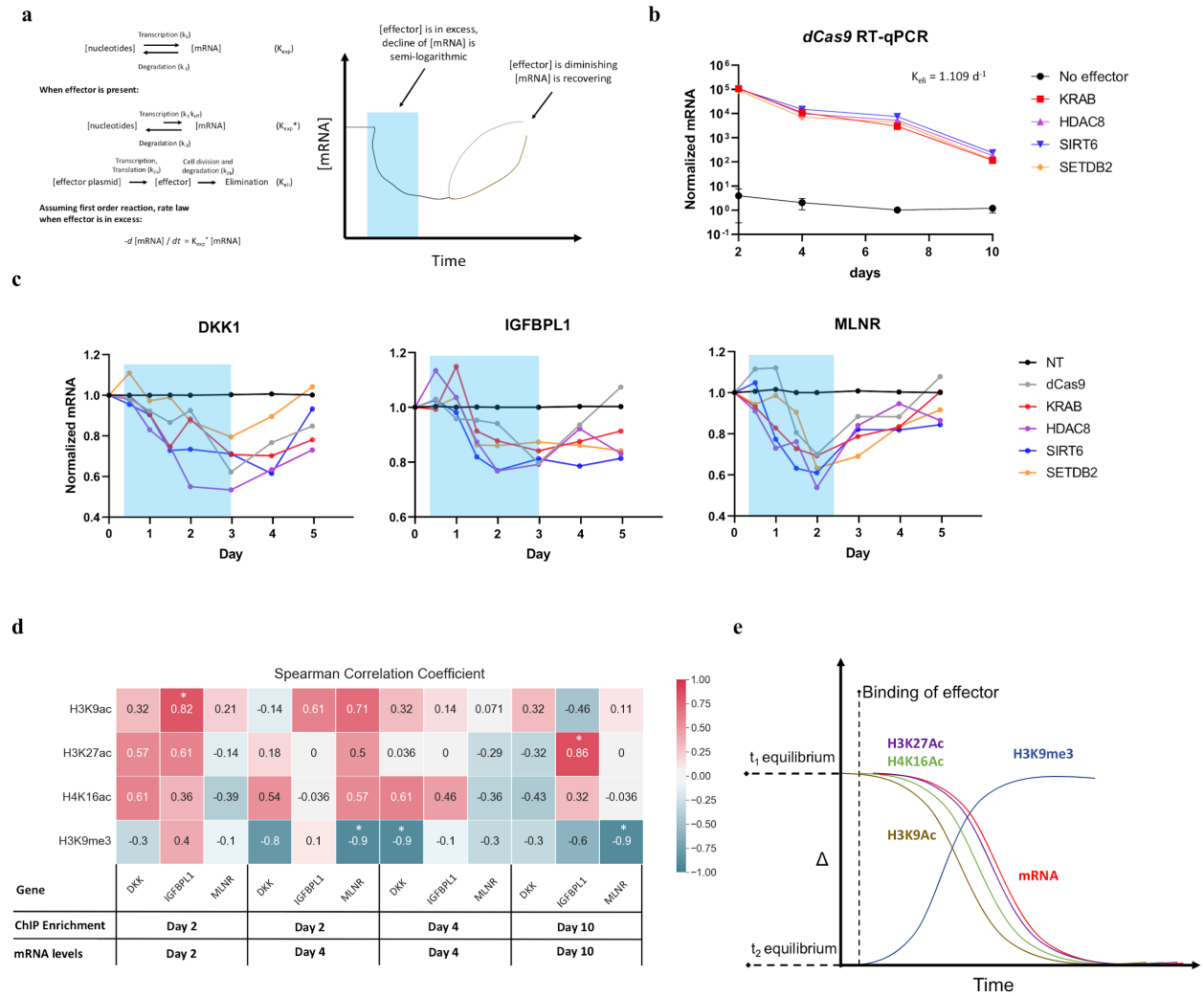


Fig. 5 Analysis of gene expression over multiple timepoints demonstrates gene- and effector-dependent kinetics and suggests that changes in histone marks may precede changes in transcription. (A) Kinetic model for gene repression by various effectors. K_{exp} denotes the unperturbed rate constant for mRNA expression, while in the presence of a repressing effector it shifts to a smaller K_{exp}^* , depending on the potency of the effector - k_{eff} . K_{eli} describes the parallel process, which is the elimination of the effector during its transient expression. When the effector is in excess, the rate law for the mRNA levels can be described by a first order logarithmic model (right). (B) Expression of dCas9 fusions 2-, 4-, 7- and 10-days post-transfection in HEK293T, demonstrating a consistent logarithmic decline of dCas9 fusions

transcript level. mRNA expression relative to non-treated cells is represented by mean \pm SEM (N=3). K_{eli} was calculated by fitting all CRISPR-GEMs measurements ($R^2 > 0.96$ for every treatment). (C) Mean mRNA levels of DKK1, IGFBPL1 and MLNR in the presence of various CRISPR-GEMs at multiple timepoints (day 0.5, 1, 1.5, 2, 3, 4 and 5; N=4, on day 2 and 4, N=2 for all other timepoints). Blue rectangles denote the region of the logarithmic phase that was used for fitting the kinetic model. (D) Spearman's rank correlation coefficients (ρ) between fold enrichment of tested histone marks and relative mRNA levels were calculated and plotted on a heatmap (for H3K9ac, H3K27ac and H4K16ac n=7, and for H3K9me3 n=5). Significance of Spearman's rank correlation analysis was calculated by a two-tailed test. * $P < 0.05$. (E) A diagram of the proposed model. The presence of CRISPR-GEMs leads to histone tail modifications that are later followed by changes in gene expression, leading to a new equilibrium. While changes in certain histone marks mildly correlate with changes in transcription, changes in H3K9 modifications correlate better with later changes in gene expression.